International Journal of Applied Information Systems (IJAIS) – ISSN : 2249-0868
Foundation of Computer Science FCS, New York, USA
Volume 3– No.4, July 2012 – www.ijais.org

Effects of Rotation and Radiation on the Hydrodynamic Flow Past an Impulsively Started Vertical Plate with Ramped Plate Temperature

M. Jana
Department of Mathematics
Vidyasagar University
Midnapore 721 102, India

S. Das
Department of Mathematics
University of Gour Banga
Malda 732 103, India

R. N. Jana
Department of Applied Mathematics
Vidyasagar University
Midnapore 721 102, India

ABSTRACT
The combined effects of rotation and radiation on the unsteady hydrodynamic flow past an impulsively accelerated vertical plate with ramped plate temperature have been studied. The fluid considered here is a gray, absorbing-emitting but non-scattering medium and the Rosseland approximation is used to describe the radiative heat flux in the analysis. An analytical solution of the governing equations has been obtained by employing the Laplace transform technique. The numerical results of fluid velocity, fluid temperature, shear stresses and the rate of heat transfer at the plate are being presented with the graphs and tables. It is observed that the radiation parameter has a retarding influence on the velocity field for the ramped plate temperature as well as the isothermal plate. An increase in radiation parameter leads to fall in the fluid temperature for the ramped plate temperature as well as the isothermal plate. Further, the rate of heat transfer at the plate increases with an increase in radiation parameter.

Keywords
Hydrodynamic flow, rotation parameter, radiation parameter, Prandtl number, Grashof number, ramped plate temperature and isothermal plate.

1. INTRODUCTION
Radiative convective flows in rotating system are encountered in countless industrial and environment processes e.g. heating and cooling chambers, fossil fuel combustion energy processes, evaporation from large open water reservoirs, astrophysical flows, solar power technology and space vehicle re-entry. Radiative heat transfer play an important role in manufacturing industries for the design of reliable equipment. Nuclear power plants, gas turbines and various propulsion device for aircraft, missiles, satellites and space vehicles are examples of such engineering applications. Das et al.[1] have studied the radiation effects on the flow past an impulsively started vertical infinite flat plate. The radiation effects on mixed convection along a vertical plate with uniform surface temperature have been investigated by Hossain and Takhar [2]. Raptis and Perdikis [3] have investigated the radiation and free convection flow past a moving plate. Revankar [4] has analyzed the free convection effect on the flow past an impulsively started or oscillating infinite vertical plate. The natural convection from a vertical flat plate with a surface temperature oscillations have been investigated by Li et al.[5]. Pathak et al.[6] have studied the effects of radiation on unsteady free convection flow bounded by an oscillating plate with variable temperature. Prasad et al. [7] have investigated the radiation and mass transfer effects on two- dimensional flow past an impulsively started infinite vertical plate. The radiation and mass transfer effects on MHD free convection flow past an impulsively started isothermal vertical plate with dissipation have been studied by Suneetha et al. [8]. Muralidharan and Muthucumaraswamy [9] have studied the thermal radiation on linearly accelerated vertical plate with variable temperature and uniform mass flux. Rajesh [10] has studied the radiation effects on MHD free convection flow near a vertical plate with ramped wall temperature. The radiation effect on natural convection near a vertical plate embedded in porous medium with ramped wall temperature have been analyzed by Das et al.[11]. Anuar et al.[12] have presented the radiation effects on the thermal boundary layer flow over a moving plate with convective boundary condition. The radiation effects on the flow past an impulsively started vertical oscillating plate with uniform heat flux have been discussed by Chandrakala [13]. Rajput and Kumar [14] have studied the effects of rotation and radiation on MHD flow past an impulsively started vertical plate with variable temperature. Seth et al.[15] have investigated the effect of rotation on unsteady hydromagnetic natural convection flow past an impulsively moving vertical plate with ramped temperature in a porous medium with thermal diffusion and heat absorption.

The aim of the present paper is to study the combined effects of rotation and radiation on unsteady hydrodynamic flow of a viscous incompressible radiative fluid past an impulsively started vertical plate with ramped plate temperature. Initially, at time $t \le 0$, both the fluid and plate are at rest with constant temperature T_∞. At time $t > 0$, the plate at $z = 0$ starts to move in its own plane with a uniform velocity u_0 and the temperature of the plate is raised or lowered to $T_w + (T_w - T_\infty)\frac{t}{t_0}$ when $0 < t \le t_0$ and the constant temperature T_w is maintained at $t > t_0$. An exact solution of the governing equations have been obtained by using the Laplace transformation technique. It is found that both the primary velocity u_1 and the absolute value of the secondary velocity v_1 decrease with an increase in radiation parameter R for the ramped plate temperature as well

as the isothermal plate. For the ramped plate temperature as well as the isothermal plate, the primary velocity u_1 and the absolute value of the secondary velocity v_1 decrease and they have oscillatory nature away from the plate with an increase in rotation parameter K^2. The primary velocity u_1 and the absolute value of the secondary velocity v_1 decrease for the ramped plate temperature while they increase for the isothermal plate with an increase in Prandtl number Pr. Both the primary velocity u_1 and the absolute value of the secondary velocity v_1 increase and they oscillate with an increase in time τ for the ramped plate temperature as well as the isothermal plate. The fluid temperature θ decreases with an increase in radiation parameter R for the ramped plate temperature as well as the isothermal plate. An increase in Prandtl number Pr leads to fall the fluid temperature θ for the ramped plate temperature as well as the isothermal plate. For the ramped plate temperature as well as the isothermal plate, the fluid temperature θ increases with an increase in time τ. The absolute value of the shear stress τ_x due to the primary flow at the plate $(\eta = 0)$ increases whereas the absolute value of the shear stress τ_y due to the secondary flow at the plate $(\eta = 0)$ decreases with an increase in radiation parameter R for the ramped plate temperature as well as isothermal plate. The absolute value of the shear stresses τ_x and τ_y increase with an increase in rotation parameter K^2. The rate of heat transfer $-\theta'(0)$ at the plate $(\eta = 0)$ increases with an increase in either Prandtl number Pr or time τ. Further, the rate of heat transfer $-\theta'(0)$ increases with an increase in radiation parameter R.

2. FORMULATION OF THE PROBLEM AND ITS SOLUTIONS

Consider the unsteady hydrodynamic flow of a viscous incompressible radiative fluid past an impulsively started vertical plate with ramped plate temperature. Choose a cartesian co-ordinates system with the x - axis along the plate in the vertically upward direction, the z - axis perpendicular to the plate and y - axis is the normal of the zx -plane [See Fig.1]. The plate and the fluid rotate in unison with uniform angular velocity Ω about z -axis. Initially, at time $t \le 0$, the plate and the fluid are assumed to be at the same temperature T_∞ and stationary. At time $t > 0$, the plate at $z = 0$ starts to move in its own plane with a uniform velocity u_0 and the temperature of the plate is raised or lowered to $T_w + (T_w - T_\infty)\frac{t}{t_0}$ when $0 < t \le t_0$ and the uniform temperature T_w is maintained when $t > t_0$. It is also assumed that the radiative heat flux in the x - direction is negligible as compared to that in the z - direction. As the plate are infinitely long, the velocity and temperature fields are functions of z and t only.

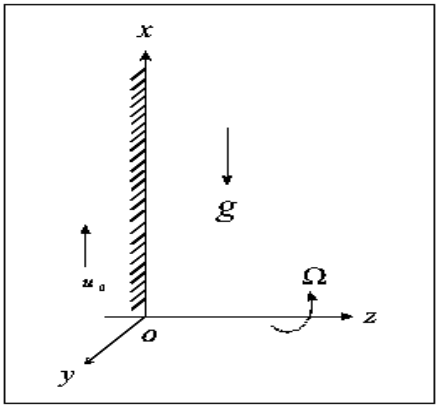

Fig 1 : Geometry of the problem

The free convection flow of a radiating fluid, under usual Boussinesq approximation, to be governed by the following system of equations

$$\frac{\partial u}{\partial t} - 2\Omega v = g\beta(T - T_\infty) + \nu\frac{\partial^2 u}{\partial z^2}, \tag{1}$$

$$\frac{\partial v}{\partial t} + 2\Omega u = \nu\frac{\partial^2 v}{\partial z^2}, \tag{2}$$

$$\rho c_p \frac{\partial T}{\partial t} = k\frac{\partial^2 T}{\partial y^2} - \frac{\partial q_r}{\partial z}, \tag{3}$$

where u and v are respectively the fluid velocity components in the x and z -directions respectively, T the temperature of the fluid, g the acceleration due to gravity, ν the kinematic coefficient of viscosity, ρ the fluid density, k the thermal conductivity, c_p the specific heat at constant pressure and q_r the radiative heat flux. The heat due to viscous dissipation is neglected for small velocities in the energy equation (3).

The initial and the boundary conditions are

$$t \le 0 : u = 0,\ v = 0,\ T = T_\infty \text{ for all } z,$$

$$t > 0 : u = u_0,\ v = 0,$$

$$T = \begin{cases} T_\infty + (T_w - T_\infty)\dfrac{t}{t_0} & \text{for } 0 < t \le t_0 \\ T_\omega & \text{for } t > t_0 \end{cases} \text{ at } z = 0, \tag{4}$$

$$t > 0 : u \to 0,\ v \to 0,\ T \to T_\infty \text{ as } z \to \infty.$$

The radiative heat flux can be found from Rosseland approximation and its formula is derived from the diffusion concept of radiative heat transfer in the following way

$$\frac{\partial q_r}{\partial z} = -4k^*\sigma(T_\infty^4 - T^4), \tag{5}$$

where σ is the Stefan-Boltzman constant and k^* the spectral mean absorption coefficient of the medium. It should be noted that by using the Rosseland approximation we limit our analysis

to optically thick fluids. If the temperature differences within the flow are sufficiently small, then the equation (5) can be linearized by expanding T^4 into the Taylor series about T_∞ and neglecting higher order terms to give:

$$T^4 = 4T_\infty^3 T - 3T_\infty^4. \qquad (6)$$

On the use of (5) and (6), equation (3) becomes

$$\rho c_p \frac{\partial T}{\partial t} = k\frac{\partial^2 T}{\partial z^2} - 16\sigma k^* T_\infty^3 (T - T_\infty). \qquad (7)$$

Introducing non-dimensionless variables

$$(u_1, v_1) \equiv \frac{(u,v)}{u_0}, \tau = \frac{t}{t_0}, \; t_0 = \frac{\nu}{u_0^2}, \eta = \frac{z u_0}{\nu}, \; \theta = \frac{T - T_\infty}{T_w - T_\infty}, \qquad (8)$$

equations (1), (2) and (7) become

$$\frac{\partial u_1}{\partial \tau} - 2K^2 v_1 = \frac{\partial^2 u_1}{\partial \eta^2} + Gr\,\theta, \qquad (9)$$

$$\frac{\partial v_1}{\partial \tau} + 2K^2 u_1 = \frac{\partial^2 v_1}{\partial \eta^2}, \qquad (10)$$

$$Pr\frac{\partial \theta}{\partial \tau} = \frac{\partial^2 \theta}{\partial \eta^2} - R\,\theta, \qquad (11)$$

where $K^2 = \frac{\Omega \nu}{u_0^2}$ is the rotation parameter, $R = \frac{16k^*\sigma T_\infty^3 \nu^2}{k u_0^2}$ the radiation parameter, $Pr = \frac{\rho \nu c_p}{k}$ the Prandtl number and $Gr = \frac{g\beta\nu(T_\omega - T_\infty)}{u_0^3}$ the Grashof number.

The corresponding initial and the boundary conditions are

$$\tau \le 0 : u_1 = 0, \; v_1 = 0, \; \theta = 0 \text{ for all } \eta,$$

$$\tau > 0 : u_1 = 1, \; v_1 = 0, \theta = \begin{cases} \tau & \text{for } 0 < \tau \le 1 \\ 1 & \text{for } \tau > 1 \end{cases} \text{at } \eta = 0,$$

(12)

$$\tau > 0 : u_1 \to 0, v_1 \to 0, \theta \to 0 \text{ as } \eta \to \infty.$$

Combining equations (9) and (10), we have

$$\frac{\partial F}{\partial \tau} + 2iK^2 F = \frac{\partial^2 F}{\partial \eta^2} + Gr\,\theta, \qquad (13)$$

where

$$F = u_1 + iv_1 \text{ and } i = \sqrt{-1}. \qquad (14)$$

The initial and the boundary conditions for $F(\eta,\tau)$ and $\theta(\eta,\tau)$ are

$$\tau \le 0 : F = 0, \; \theta = 0 \text{ for all } \eta,$$

$$\tau > 0 : F = 1, \; \theta = \begin{cases} \tau & \text{for } 0 < \tau \le 1 \\ 1 & \text{for } \tau > 1 \end{cases} \text{at } \eta = 0,$$

(15)

$$\tau > 0 : F \to 0, \; \theta \to 0 \text{ as } \eta \to \infty.$$

On the use of Laplace transformation, equations (13) and (11) become

$$(s + 2iK^2)\bar{F} = \frac{d^2\bar{F}}{d\eta^2} + Gr\,\bar{\theta},$$

(16)

$$Prs\,\bar{\theta} = \frac{d^2\bar{\theta}}{d\eta^2} - R\bar{\theta},$$

(17)

where

$$\bar{F}(\eta,s) = \int_0^\infty F(\eta,\tau)e^{-s\tau}\,d\tau, \; \bar{\theta}(\eta,s) = \int_0^\infty \theta(\eta,\tau)e^{-s\tau}\,d\tau.$$

(18)

The corresponding boundary conditions for $\bar{F}$ and $\bar{\theta}$ are

$$\bar{F} = \frac{1}{s}, \; \bar{\theta} = \frac{1}{s^2}(1 - e^{-s}) \text{ at } \eta = 0,$$

$$\bar{F} \to 0, \; \bar{\theta} \to 0 \text{ as } \eta \to \infty. \qquad (19)$$

The solution of the equations (16) and (17) subject to the boundary conditions (19) are easily obtained and are given by

$$\bar{\theta}(\eta,s) = \begin{cases} \frac{\left(1 - e^{-s}\right)}{s^2} \; e^{-\sqrt{R+Prs}\;\eta} & \text{for } Pr \ne 1, \\ \frac{\left(1 - e^{-s}\right)}{s^2} \; e^{-\sqrt{R+s}\;\eta} & \text{for } Pr = 1 \end{cases} \qquad (20)$$

$$\bar{F}(\eta,s) = \begin{cases} \frac{e^{-\sqrt{s+2iK^2}\;\eta}}{s} + \frac{Gr(1-e^{-s})}{s^2(Pr-1)(s-\beta_0)}\left[e^{-\sqrt{s+2iK^2}\;\eta} - e^{-\sqrt{R+sPr}\;\eta}\right] & \text{for } Pr \ne 1, \\ \frac{e^{-\sqrt{s+2iK^2}\;\eta}}{s} + \frac{Gr(1-e^{-s})}{s^2(R-2iK^2)}\left[e^{-\sqrt{s+2iK^2}\;\eta} - e^{-\sqrt{R+s}\,\eta}\right] & \text{for } Pr = 1, \end{cases} \qquad (21)$$

where $\beta_0 = \dfrac{R-2iK^2}{1-Pr}$.

The inverse Laplace transforms of (20) and (21) give the solution for the temperature distribution and velocity field as

$$\theta(\eta,\tau) = \begin{cases} F_1(\eta,R,Pr,\tau) - H(\tau-1)F_1(\eta,R,Pr,\tau-1) & \text{for } Pr \neq 1, \\ F_5(\eta,R,\tau) - H(\tau-1)F_5(\eta,R,\tau-1) & \text{for } Pr = 1, \end{cases} \tag{22}$$

$$F(\eta,\tau) = \begin{cases} F_4(\eta,2iK^2,\tau) + \dfrac{Gr}{Pr-1}\Big[F_3(\eta,\beta_0,2iK^2,\tau) - F_2(\eta,\beta_0,R,Pr,\tau) \\ -H(\tau-1)\{F_3(\eta,\beta_0,2iK^2,\tau-1) - F_2(\eta,\beta_0,R,Pr,\tau-1)\}\Big] & \text{for } Pr \neq 1, \\ F_4(\eta,2iK^2,\tau) + \dfrac{Gr}{R-2iK^2}\Big[F_6(\eta,2iK^2,\tau) - F_5(\eta,R,\tau) \\ -H(\tau-1)\{F_6(\eta,2iK^2,\tau-1) - F_5(\eta,R,\tau-1)\}\Big] & \text{for } Pr = 1, \end{cases} \tag{23}$$

where

$$F_1(\eta,R,Pr,\tau) = \frac{1}{2}\left[\left(\tau + \frac{Pr\eta}{2\sqrt{R}}\right)e^{\eta\sqrt{R}}\operatorname{erfc}\left(\frac{\eta\sqrt{Pr}}{2\sqrt{\tau}} + \sqrt{\frac{R\tau}{Pr}}\right) + \left(\tau - \frac{Pr\eta}{2\sqrt{R}}\right)e^{-\eta\sqrt{R}}\operatorname{erfc}\left(\frac{\eta\sqrt{Pr}}{2\sqrt{\tau}} - \sqrt{\frac{R\tau}{Pr}}\right)\right],$$

$$\begin{aligned} F_2(\eta,R,Pr,\beta_0,\tau) = &-\left\{\frac{1}{2\beta_0}\left(\tau + \frac{\eta Pr}{2\sqrt{R}}\right) + \frac{1}{2\beta_0^2}\right\}e^{\sqrt{R}\eta}\operatorname{erfc}\left(\frac{\eta\sqrt{Pr}}{2\sqrt{\tau}} + \sqrt{\frac{R\tau}{Pr}}\right) \\ &-\left\{\frac{1}{2\beta_0}\left(\tau - \frac{\eta Pr}{2\sqrt{R}}\right) + \frac{1}{2\beta_0^2}\right\}e^{-\sqrt{R}\eta}\operatorname{erfc}\left(\frac{\eta\sqrt{Pr}}{2\sqrt{\tau}} - \sqrt{\frac{R\tau}{Pr}}\right) \\ &+\frac{e^{\beta_0\tau}}{2\beta_0^2}\left[e^{\sqrt{R+Pr\beta_0}\,\eta}\operatorname{erfc}\left\{\frac{\eta\sqrt{Pr}}{2\sqrt{\tau}} + \sqrt{\left(\frac{R}{Pr}+\beta_0\right)\tau}\right\} + e^{-\sqrt{R+Pr\beta_0}\,\eta}\operatorname{erfc}\left\{\frac{\eta\sqrt{Pr}}{2\sqrt{\tau}} - \sqrt{\left(\frac{R}{Pr}+\beta_0\right)\tau}\right\}\right], \end{aligned} \tag{24}$$

$$\begin{aligned} F_3(\eta,\beta_0,2iK^2,\tau) = &-\left\{\frac{1}{2\beta_0}\left(\tau + \frac{\eta}{2\sqrt{2iK^2}}\right) + \frac{1}{2\beta_0^2}\right\}e^{\sqrt{2iK^2}\,\eta}\operatorname{erfc}\left(\frac{\eta}{2\sqrt{\tau}} + \sqrt{2iK^2\tau}\right) \\ &-\left\{\frac{1}{2\beta_0}\left(\tau - \frac{\eta}{2\sqrt{2iK^2}}\right) + \frac{1}{2\beta_0^2}\right\}e^{-\sqrt{2iK^2}\,\eta}\operatorname{erfc}\left(\frac{\eta}{2\sqrt{\tau}} - \sqrt{2iK^2\tau}\right) \\ &+\frac{e^{\beta_0\tau}}{2\beta_0^2}\left[e^{\sqrt{2iK^2+\beta_0}\,\eta}\operatorname{erfc}\left(\frac{\eta}{2\sqrt{\tau}} + \sqrt{(2iK^2+\beta_0)\tau}\right) + e^{-\sqrt{2iK^2+\beta_0}\,\eta}\operatorname{erfc}\left\{\frac{\eta}{2\sqrt{\tau}} - \sqrt{(2iK^2+\beta_0)\tau}\right\}\right], \end{aligned}$$

$$F_4(\eta,2iK^2,\tau) = \frac{1}{2}\left[e^{\sqrt{2iK^2}\,\eta}\operatorname{erfc}\left(\frac{\eta}{2\sqrt{\tau}} + \sqrt{2iK^2\tau}\right) + e^{-\sqrt{2iK^2}\,\eta}\operatorname{erfc}\left(\frac{\eta}{2\sqrt{\tau}} - \sqrt{2iK^2\tau}\right)\right],$$

$$F_5(\eta,R,\tau) = \frac{1}{2}\left[\left(\tau + \frac{\eta}{2\sqrt{R}}\right)e^{\eta\sqrt{R}}\operatorname{erfc}\left(\frac{\eta}{2\sqrt{\tau}} + \sqrt{R\tau}\right) + \left(\tau - \frac{\eta}{2\sqrt{R}}\right)e^{-\eta\sqrt{R}}\operatorname{erfc}\left(\frac{\eta}{2\sqrt{\tau}} - \sqrt{R\tau}\right)\right],$$

$$F_6(\eta,2iK^2,\tau) = \frac{1}{2}\left[\left(\tau + \frac{\eta}{2\sqrt{2iK^2}}\right)e^{\eta\sqrt{2iK^2}}\operatorname{erfc}\left(\frac{\eta}{2\sqrt{\tau}} + \sqrt{2iK^2\tau}\right) + \left(\tau - \frac{\eta}{2\sqrt{2iK^2}}\right)e^{-\eta\sqrt{2iK^2}}\operatorname{erfc}\left(\frac{\eta}{2\sqrt{\tau}} - \sqrt{2iK^2\tau}\right)\right]$$

and F_1, F_2, F_3, F_4, F_5 and F_6 are dummy functions and $\operatorname{erfc}(.)$ being complementary error function and $H(\tau-1)$ is the Heaviside unit step function.

2.1. Solution for isothermal plate

In order to highlight the effects of the ramped temperature distribution near the plate on the fluid flow, it may be meaningful to compare such a flow with the one near a moving plate with uniform temperature. Taking into consideration the assumptions made in this problem, the solution for the fluid temperature and velocity for the flow near an impulsively moving vertical isothermal plate is obtained. In this case, the initial and boundary conditions for the temperature and velocity fields are

$$u = 0,\ v = 0,\ T = T_\infty \quad \text{for all } z \text{ and } t \le 0,$$

$$u = u_0,\ v = 0,\ T = T_w \text{ at } z = 0 \text{ for } t > 0, \qquad (25)$$
$$u \to 0,\ v \to 0,\ T \to T_\infty \text{ as } z \to \infty \text{ for } t > 0.$$

On the use of (8), the boundary conditions (25) become

$$u_1 = 0,\ v_1 = 0,\ \theta = 0 \text{ for all } \eta \text{ and } \tau \le 0,$$
$$u_1 = 1,\ v_1 = 0,\ \theta = 1 \text{ at } \eta = 0 \text{ for } \tau > 0, \qquad (26)$$
$$u_1 \to 0,\ v_1 \to 0,\ \theta \to 0 \text{ as } \eta \to \infty \text{ for } \tau > 0.$$

The corresponding boundary conditions for $\bar{\theta}$ and $\bar{F}$ are

$$\bar{F} = \frac{1}{s},\ \bar{\theta} = \frac{1}{s} \text{ at } \eta = 0,$$
$$\bar{F} \to 0,\ \bar{\theta} \to 0 \text{ as } \eta \to \infty. \qquad (27)$$

The solution of the equations (16) and (17) subject to the boundary conditions (27) are given by

$$\bar{\theta}(\eta, s) = \begin{cases} \dfrac{e^{-\sqrt{R+Prs}\,\eta}}{s} & \text{for } Pr \neq 1, \\ \dfrac{e^{-\sqrt{R+s}\,\eta}}{s} & \text{for } Pr = 1, \end{cases} \qquad (28)$$

$$\bar{F}(\eta, s) = \begin{cases} \dfrac{e^{-\sqrt{s+2iK^2}\,\eta}}{s} + \dfrac{Gr}{(Pr-1)\beta_0}\left(\dfrac{1}{s-\beta_0} - \dfrac{1}{s}\right)\left[e^{-\sqrt{s+2iK^2}\,\eta} - e^{-\sqrt{R+Prs}\,\eta}\right] & \text{for } Pr \neq 1, \\ \dfrac{e^{-\sqrt{s+2iK^2}\,\eta}}{s} + \dfrac{Gr}{(R-2iK^2)s}\left[e^{-\sqrt{s+2iK^2}\,\eta} - e^{-\sqrt{R+s}\,\eta}\right] & \text{for } Pr = 1. \end{cases} \qquad (29)$$

The inverse transforms of equations (28) and (29) give the solution for the temperature distribution and velocity field as

$$\theta(\eta, \tau) = \begin{cases} F_7(\eta, R, Pr, \tau) & \text{for } Pr \neq 1, \\ F_8(\eta, R, \tau) & \text{for } Pr = 1, \end{cases} \qquad (30)$$

$$F(\eta, \tau) = \begin{cases} F_4(\eta, 2iK^2, \tau) + \dfrac{Gr}{\beta_0(Pr-1)}\Big[F_{10}(\eta, 2iK^2, \beta_0, \tau) - F_9(\eta, R, Pr, \beta_0, \tau) \\ \quad -\{F_{10}(\eta, 2iK^2, \tau) - F_9(\eta, R, Pr, \tau)\}\Big] & \text{for } Pr \neq 1, \\ F_4(\eta, 2iK^2, \tau) + \dfrac{Gr}{R-2iK^2}\Big[F_4(\eta, 2iK^2, \tau) - F_8(\eta, R, \tau)\Big] & \text{for } Pr = 1, \end{cases} \qquad (31)$$

where

$$F_7(\eta, R, Pr, \tau) = \frac{1}{2}\left[e^{\eta\sqrt{R}}\operatorname{erfc}\left(\frac{\eta\sqrt{Pr}}{2\sqrt{\tau}} + \sqrt{\frac{R\tau}{Pr}}\right) + e^{-\eta\sqrt{R}}\operatorname{erfc}\left(\frac{\eta\sqrt{Pr}}{2\sqrt{\tau}} - \sqrt{\frac{R\tau}{Pr}}\right)\right],$$

$$F_8(\eta, R, \tau) = \frac{1}{2}\left[e^{\eta\sqrt{R}}\operatorname{erfc}\left(\frac{\eta}{2\sqrt{\tau}} + \sqrt{R\tau}\right) + e^{-\eta\sqrt{R}}\operatorname{erfc}\left(\frac{\eta}{2\sqrt{\tau}} - \sqrt{R\tau}\right)\right],$$

$$F_9(\eta, R, Pr, \beta_0, \tau) = \frac{1}{2}e^{\beta_0\tau}\left[e^{\sqrt{R+Pr\beta_0}\,\eta}\operatorname{erfc}\left\{\frac{\eta\sqrt{Pr}}{2\sqrt{\tau}} + \sqrt{\left(\frac{R}{Pr} + \beta_0\right)\tau}\right\}\right.$$
$$\left. + e^{-\sqrt{R+Pr\beta_0}\,\eta}\operatorname{erfc}\left\{\frac{\eta\sqrt{Pr}}{2\sqrt{\tau}} - \sqrt{\left(\frac{R}{Pr} + \beta_0\right)\tau}\right\}\right], \qquad (32)$$

$$F_{10}(\eta, \beta_0, 2iK^2, \tau) = \frac{1}{2}e^{\beta_0\tau}\left[e^{\sqrt{2iK^2+\beta_0}\,\eta}\operatorname{erfc}\left\{\frac{\eta}{2\sqrt{\tau}} + \sqrt{(2iK^2+\beta_0)\tau}\right\} + e^{-\sqrt{2iK^2+\beta_0}\,\eta}\operatorname{erfc}\left\{\frac{\eta}{2\sqrt{\tau}} - \sqrt{(2iK^2+\beta_0)\tau}\right\}\right]$$

and F_7, F_8, F_9 and F_{10} are dummy functions.

3. RESULTS AND DISCUSSION

We have presented the non-dimensional velocity components u_1 and v_1 and the fluid temperature θ for several values of the radiation parameter R, rotation parameter K^2, Grashof number Gr, Prandtl number Pr and time τ in Figs.2-14. It is seen from Figs.2 and 3 that both the primary velocity u_1 and the absolute value of the secondary velocity v_1 decrease with an increase in radiation parameter R for the ramped plate temperature as well as the isothermal plate. This means that in the presence of radiation the velocity field retards. Figs.4 and 5 illustrate that the primary velocity u_1 decreases whereas the absolute value of the secondary velocity v_1 increases near the plate and they have oscillatory nature away from the plate with an increase in rotation parameter K^2 for the ramped plate temperature as well as the isothermal plate. This implies that rotation retards the primary velocity whereas it accelerates the secondary velocity. This may be attributed to the fact that when the frictional layer near the plate is suddenly set into motion then the Coriolis force acts as a constraint in the main fluid flow to induce cross flow in the flow field. It is revealed from Figs.6 and 7 that both the primary velocity u_1 and the absolute value of the secondary velocity v_1 decrease for the ramped plate temperature while they increase for the isothermal plate with an increase in Prandtl number Pr. This is due to the fact that the fluids with high Prandtl number have greater viscosity, which makes the fluid thick and hence move slowly. Figs.8 and 9 show that both the primary velocity u_1 and the absolute value of the secondary velocity increase with an increase in Grashof number Gr for the ramped plate temperature as well as the isothermal plate. Grashof number Gr signifies the relative effects of thermal buoyancy force to the viscous hydrodynamic force in the boundary layer. As expected, it is observed that, for both ramped temperature and isothermal plate, the primary and secondary velocities increase on increasing Gr which implies that there is a rise in both the velocities due to enhancement of thermal buoyancy force. Figs. 10 and 11 display that both the primary velocity u_1 and the absolute value of the secondary velocity v_1 increase near the plate while they decrease away from the plate with an increase in time τ for the ramped plate temperature as well as the isothermal plate. Fig.12 reveals that the fluid temperature θ decreases with an increase in radiation parameter R for the ramped plate temperature as well as the isothermal plate. In the presence of radiation, the thermal boundary layer always found to thicken which implies that the radiation provides an additional means to diffuse energy. This means that the thermal boundary layer decreases and more uniform temperature distribution across the boundary layer. It is found from Fig.13 that the fluid temperature θ decreases with an increase in Prandtl number Pr for the ramped plate temperature as well as the isothermal plate. Fig.14 displays that the fluid temperature θ increases with an increase in time τ for the ramped plate temperature as well as the isothermal plate. As time progresses there is a rise in fluid temperature for both ramped temperature and isothermal plate. It may be noted from Figs. 2 to 11 that the fluid velocities are faster in the case of isothermal plate than that in the case of ramped temperature plate. Figs.12 to 14 show that the fluid temperature is less in the case of ramped temperature plate than that in the case of isothermal plate.

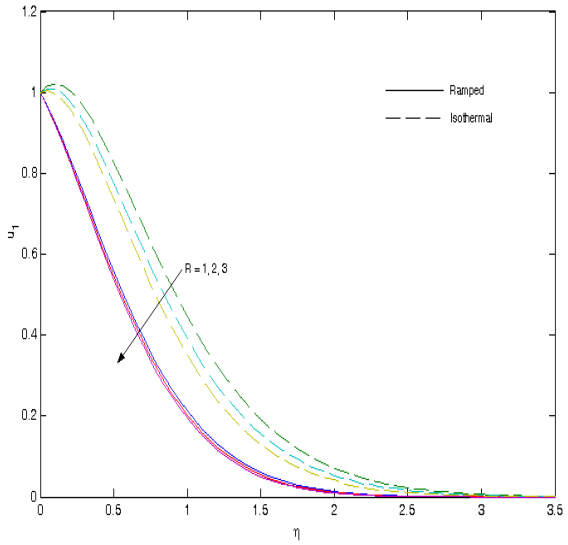

Fig 2: Primary velocity u_1 for different R when $Pr = 0.71$, $Gr = 5$, $K^2 = 2$ and $\tau = 0.5$

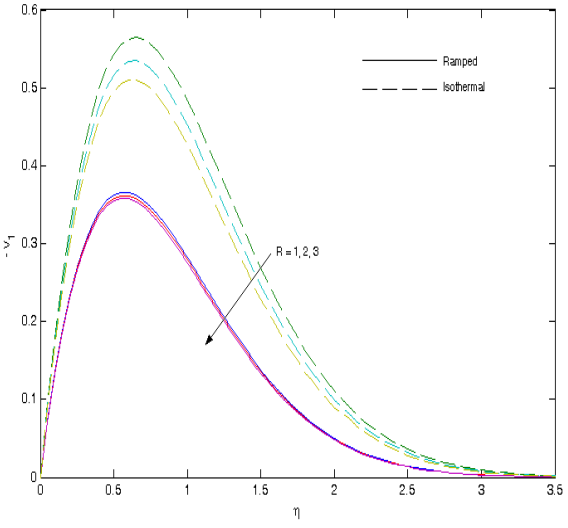

Fig 3: Secondary velocity v_1 for different R when $Pr = 0.71$, $Gr = 5$, $K^2 = 2$ and $\tau = 0.5$

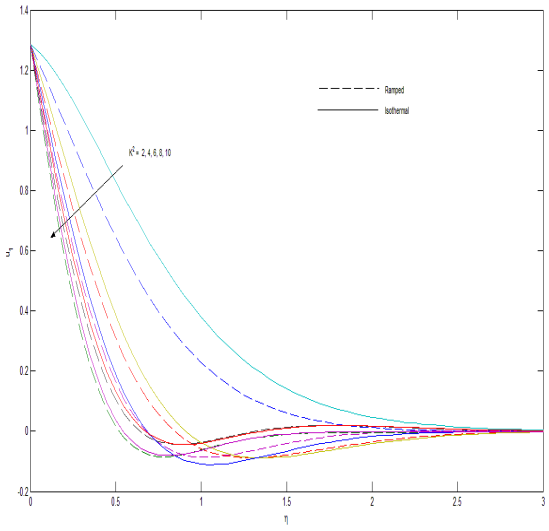

Fig 4: Primary velocity u_1 for different K^2 when $Pr = 0.71$, $Gr = 5$, $R = 2$ and $\tau = 0.5$

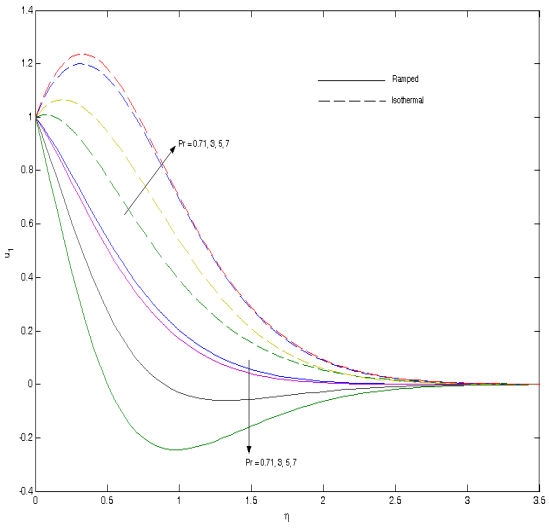

Fig 6: Primary velocity u_1 for different Pr when $Gr = 5$, $K^2 = 2$, $R = 2$ and $\tau = 0.5$

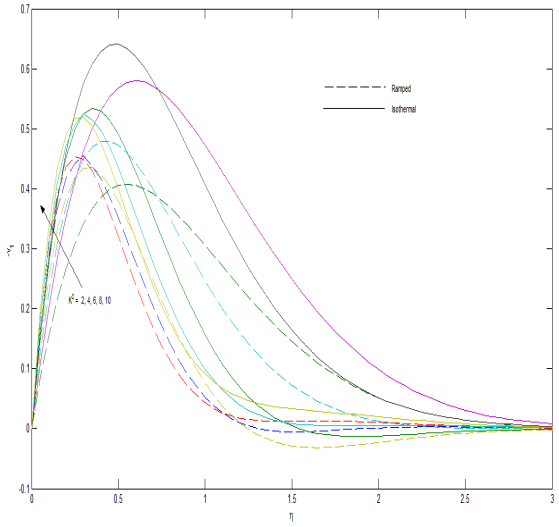

Fig 5: Secondary velocity v_1 for different K^2 when $Pr = 0.71$, $Gr = 5$, $R = 2$ and $\tau = 0.5$

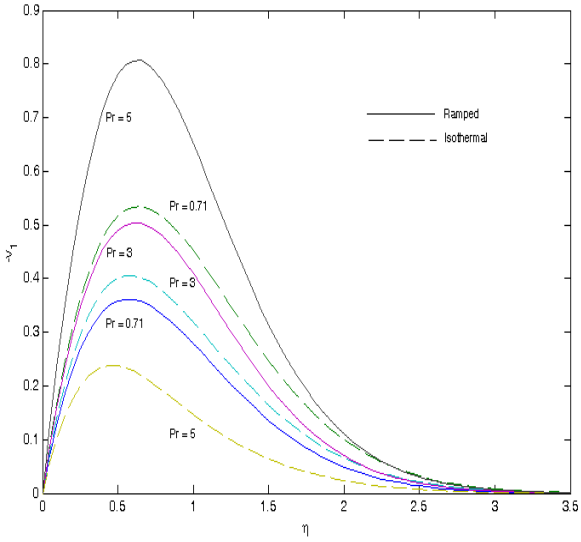

Fig 7: Secondary velocity v_1 for different Pr, when $Gr = 5$, $K^2 = 2$, $R = 2$ and $\tau = 0.5$

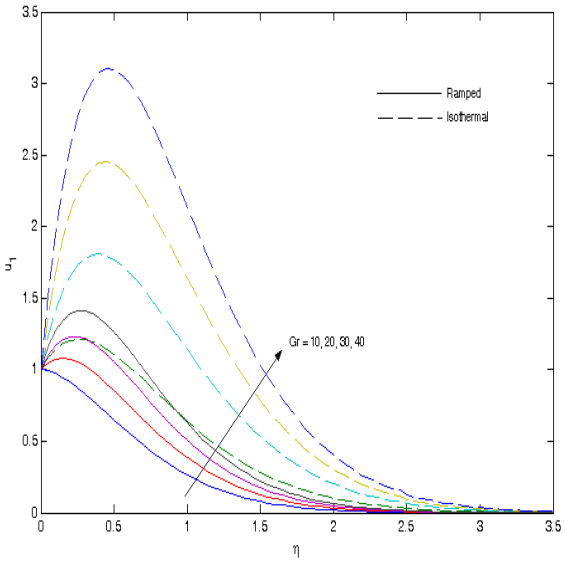

Fig 8: Primary velocity u_1 for different Gr when $Pr = 0.71$, $K^2 = 2$, $R = 2$ and $\tau = 0.5$

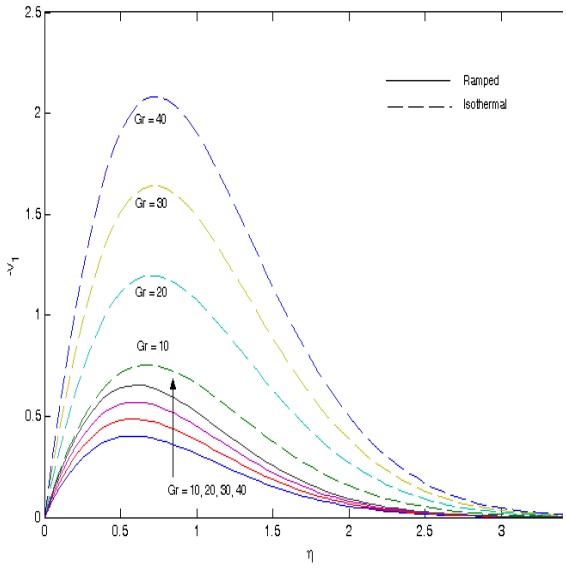

Fig 9: Secondary velocity v_1 for different Gr when $Pr = 0.71$, $K^2 = 2$, $R = 2$ and $\tau = 0.5$

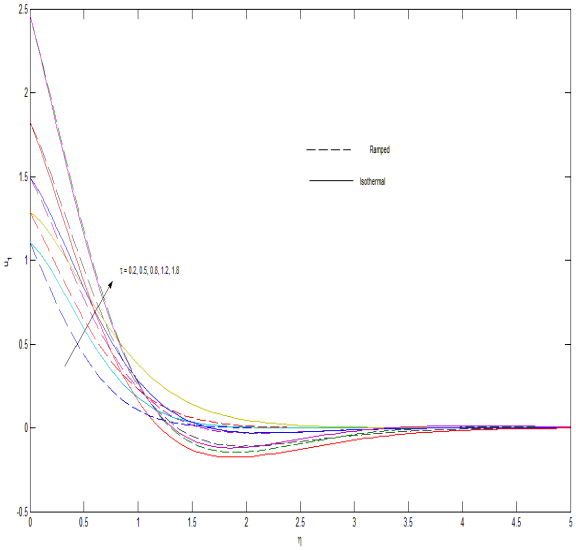

Fig 10: Primary velocity u_1 for different τ when $Pr = 0.71$, $Gr = 5$, $K^2 = 2$ and $R = 2$

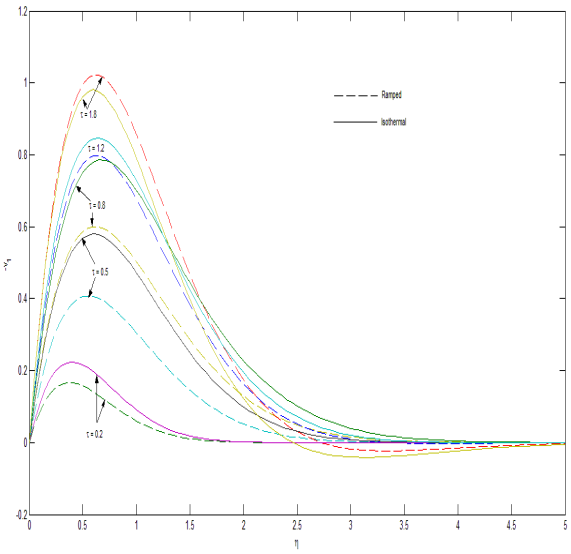

Fig 11: Secondary velocity v_1 for different τ when $Pr = 0.71$, $Gr = 5$, $K^2 = 2$ and $R = 2$

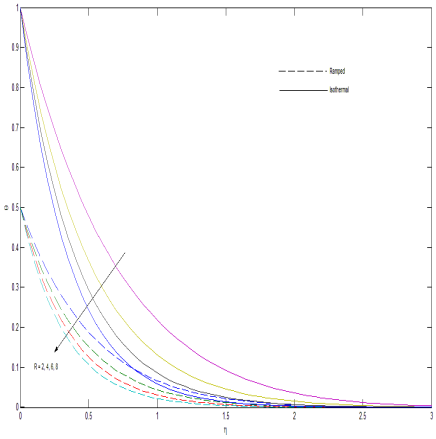

Fig 12: Temperature θ for different R when $Pr = 0.71$ and $\tau = 0.5$

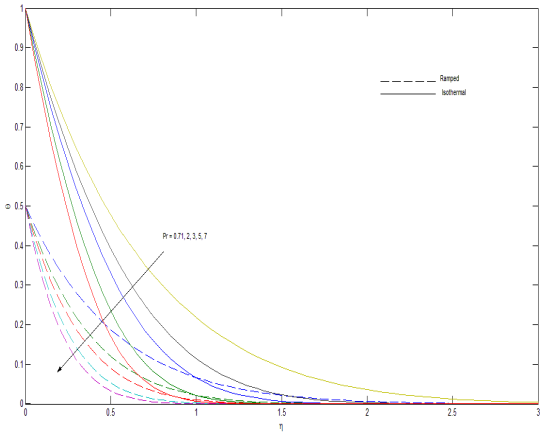

Fig 13: Temperature θ for different Pr when $R = 2$ and $\tau = 0.5$

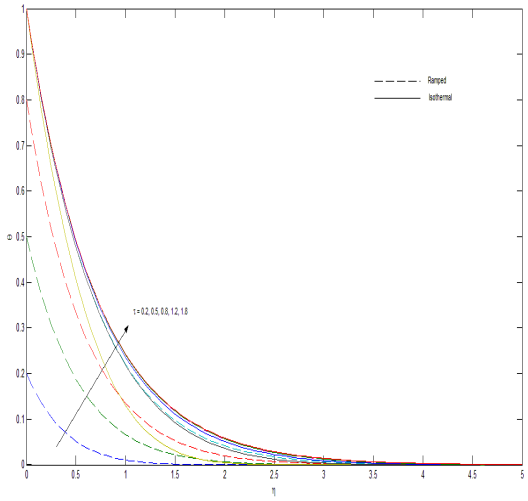

Fig 14: Temperature θ for different τ when $Pr = 0.71$ and $R = 2$

For ramped plate temperature, the rate of heat transfer and the non-dimensional shear stresses due the primary and the secondary flows at the plate $\eta = 0$ are given by

$$-\left(\frac{\partial\theta}{\partial\eta}\right)_{\eta=0} = \begin{cases} G_1(Pr,R,\tau) - H(\tau-1)G_1(Pr,R,\tau-1) & \text{for } Pr \neq 1, \\ G_5(R,\tau) - H(\tau-1)G_5(R,\tau-1) & \text{for } Pr = 1, \end{cases} \tag{33}$$

$$\tau_x + i\tau_y = \left(\frac{\partial F}{\partial\eta}\right)_{\eta=0}$$

$$= \begin{cases} -G_4(2iK^2,\tau) + \dfrac{Gr}{Pr-1}\Big[G_3(\beta_0,2iK^2,\tau) - G_2(\beta_0,R,Pr,\tau) \\ -H(\tau-1)\{G_3(\beta_0,2iK^2,\tau-1) - G_2(\beta_0,R,Pr,\tau-1)\}\Big] & \text{for } Pr \neq 1, \\ -G_4(2iK^2,\tau) - \dfrac{Gr}{R-2iK^2}\Big[G_6(2iK^2,\tau) - G_5(R,\tau) \\ -H(\tau-1)\{G_6(2iK^2,\tau-1) - G_5(R,\tau-1)\}\Big] & \text{for } Pr = 1, \end{cases} \tag{34}$$

where

$$G_1(Pr,R,\tau)=\left(\frac{Pr}{2\sqrt{R}}+\tau\sqrt{R}\right)\text{erf}\left(\sqrt{\frac{R\tau}{Pr}}\right)+\sqrt{\frac{Pr\,\tau}{\pi}}\,e^{-\frac{R\tau}{\text{Pr}}},$$

$$G_2(R,Pr,\beta_0,\tau)=\left[\left\{\frac{Pr}{2\beta_0\sqrt{R}}+\sqrt{R}\left(\frac{\tau}{\beta_0}+\frac{1}{\beta_0^2}\right)\right\}\text{erf}\left(\sqrt{\frac{R\tau}{Pr}}\right)+\left(\frac{\tau}{\beta_0}+\frac{1}{\beta_0^2}\right)\sqrt{\frac{Pr}{\pi\tau}}\,e^{-\frac{R\tau}{\text{Pr}}}\right]$$

$$-\frac{e^{\beta_0\tau}}{\beta_0^2}\left[\sqrt{R+Pr\beta_0}\ \text{erf}\left\{\sqrt{\left(\frac{R}{Pr}+\beta_0\right)\tau}\right\}+\frac{1}{\sqrt{\pi\tau}}\,e^{-\left(\frac{R}{Pr}+\beta_0\right)\tau}\right], \tag{35}$$

$$G_3(\beta_0,2iK^2,\tau)=\left[\left\{\frac{1}{2\beta_0\sqrt{2iK^2}}+\sqrt{2iK^2}\left(\frac{\tau}{\beta_0}+\frac{1}{\beta_0^2}\right)\right\}\text{erf}\left(\sqrt{2iK^2\tau}\right)+\left(\frac{\tau}{\beta_0}+\frac{1}{\beta_0^2}\right)\frac{1}{\sqrt{\pi\tau}}e^{-2iK^2\tau}\right]$$

$$-\frac{e^{\beta_0\tau}}{\beta_0^2}\left[\sqrt{\beta_0+2iK^2}\ \text{erf}\left\{\sqrt{(\beta_0+2iK^2)\tau}\right\}+\frac{1}{\sqrt{\pi\tau}}\,e^{-\left(\beta_0+2iK^2\right)\tau}\right],$$

$$G_4(2iK^2,\tau)=\left[\sqrt{2iK^2}\ \text{erf}\left(\sqrt{2iK^2\tau}\right)+\frac{1}{\sqrt{\pi\tau}}\,e^{-2iK^2\tau}\right],$$

$$G_5(R,\tau)=\left(\frac{1}{2\sqrt{R}}+\tau\sqrt{R}\right)\text{erf}\left(\sqrt{R\tau}\right)+\sqrt{\frac{\tau}{\pi}}e^{-R\tau},$$

$$G_6(2iK^2,\tau)=\left(\frac{1}{2\sqrt{2iK^2}}+\tau\sqrt{2iK^2}\right)\text{erf}\left(\sqrt{2iK^2\tau}\right)+\sqrt{\frac{\tau}{\pi}}e^{-2iK^2\tau}$$

and G_1, G_2, G_3, G_4, G_5 and G_6 are dummy functions.

For isothermal plate, the rate of heat transfer and the non-dimensional shear stresses due to the primary and the secondary flows at the plate $\eta=0$ are obtained as

$$-\left(\frac{\partial\theta}{\partial\eta}\right)_{\eta=0}=\begin{cases}G_7(R,Pr,\tau) & \text{for } Pr\neq 1,\\ G_8(R,\tau) & \text{for } Pr=1,\end{cases} \tag{36}$$

$$\tau_x+i\tau_y=\left(\frac{\partial F}{\partial\eta}\right)_{\eta=0}$$

$$=\begin{cases}-G_4(2iK^2,\tau)-\dfrac{Gr}{\beta_0(Pr-1)}\Big[G_{10}(2iK^2,\beta_0,\tau)-G_9(R,Pr,\beta_0,\tau) & \\ \quad -\{G_4(2iK^2,\tau)-G_7(R,Pr,\tau)\}\Big] & \text{for } Pr\neq 1,\\ -G_4(2iK^2,\tau)-\dfrac{Gr}{R-2iK^2}\Big[G_4(2iK^2,\tau)-G_8(R,\tau)\Big] & \text{for } Pr=1,\end{cases} \tag{37}$$

where

$$G_7(R,Pr,\tau)=\left[\sqrt{R}\ erf\left(\sqrt{\frac{R\tau}{Pr}}\right)+\sqrt{\frac{Pr}{\pi\,\tau}}\ e^{-R\,\tau/Pr}\right],$$

$$G_8(R,\tau)=\left[\sqrt{R}\ erf\left(\sqrt{R\tau}\right)+\frac{1}{\sqrt{\pi\tau}}\,e^{-R\tau}\right],$$

$$G_9(R,Pr,\beta_0,\tau)=e^{\beta_0\tau}\left[\sqrt{R+Pr\beta_0}\ erf\left\{\sqrt{\left(\frac{R}{Pr}+\beta_0\right)\tau}\right\}+\sqrt{\frac{Pr}{\pi\tau}}\ e^{-\left(\frac{R}{Pr}+\beta_0\right)\tau}\right], \tag{38}$$

$$G_{10}(\beta_0, 2iK^2, \tau) = e^{\beta_0 \tau}\left[\sqrt{2iK^2+\beta_0}\ erf\left\{\sqrt{(2iK^2+\beta_0)\tau}\right\} + \frac{1}{\sqrt{\pi\tau}}e^{-(2iK^2+\beta_0)\tau}\right]$$

and G_7, G_8, G_9, G_{10} are dummy functions.

Numerical results of the rate of heat transfer $-\theta'(0)$ at the plate $(\eta = 0)$ against the radiation parameter R are presented in the Table 1 for several values of Prandtl number Pr and time τ. Table 1 shows that for the fixed value of radiation parameter R, the rate of heat transfer $-\theta'(0)$ increases with an increase in either Prandtl number Pr or time τ. This may be explained by the fact that the frictional forces become dominant with increasing values of Pr and hence yield greater heat transfer rate. As time progresses there is a rise in the rate of heat transfer. Further, it is observed that for fixed value of Pr and τ, the rate of heat transfer $-\theta'(0)$ increases with an increase in radiation parameter R. Thus, the thermal radiation accelerates the heat transfer rate at the plate.

Table 1. Rate of heat transfer $-\theta'(0)$ at the plate $\eta = 0$.

	Pr				τ			
R	0.71	2	3	7	0.3	0.7	0.9	1.2
2	0.95094	1.30760	1.53055	2.20993	0.65638	1.23794	1.52246	1.54678
4	1.17685	1.47156	1.67032	2.30638	0.77423	1.57735	1.97747	2.00810
6	1.36959	1.62288	1.80229	2.40026	0.87899	1.85956	2.34947	2.45216
8	1.53971	1.76367	1.92739	2.49174	0.97382	2.10541	2.67110	2.82943

Numerical values of the non-dimensional shear stress τ_x due to the primary flow and shear stress τ_y due to the secondary flow at the plate $(\eta = 0)$ are presented in Figs.15-20 against Grashof number Gr for several values of radiation parameter R, rotation parameter K^2 and Prandtl number Pr when $\tau = 0.5$. Figs.15 and 16 show that for the fixed values of the Grashof number Gr, the absolute value of shear stress τ_x increases whereas the absolute value of the shear stress τ_y decreases with an increase in radiation parameter R for the ramped plate temperature as well as isothermal plate. On other hand, it is observed that the absolute value of the shear stress τ_x decreases whereas the absolute value of the shear stress τ_y increases with an increase in Grashof number Gr for the fixed values of the radiation parameter R. Figs.17 and 18 reveal that the absolute value of both the shear stresses τ_x and τ_y increase with an increase in rotation parameter K^2. This implies that, for both ramped temperature and isothermal plate, rotation tends to increase shear stress. It is seen from Figs.19 and 20 that the absolute value of both the shear stresses τ_x and τ_y increase with an increase in Prandtl number Pr.

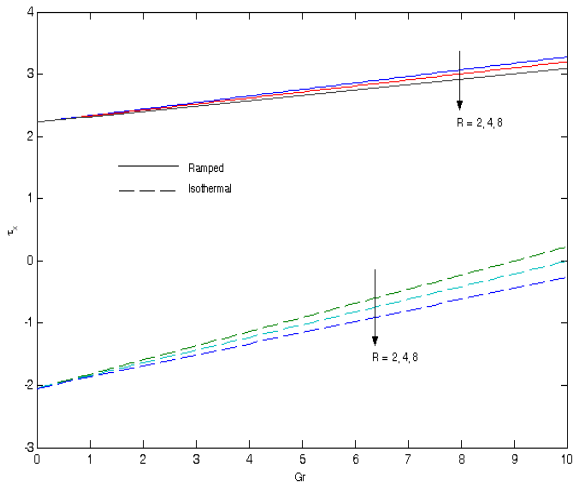

Fig 15: Shear stress τ_x for different R when $Pr = 0.71$, $K^2 = 2$, $\tau = 0.5$ and $Gr = 5$

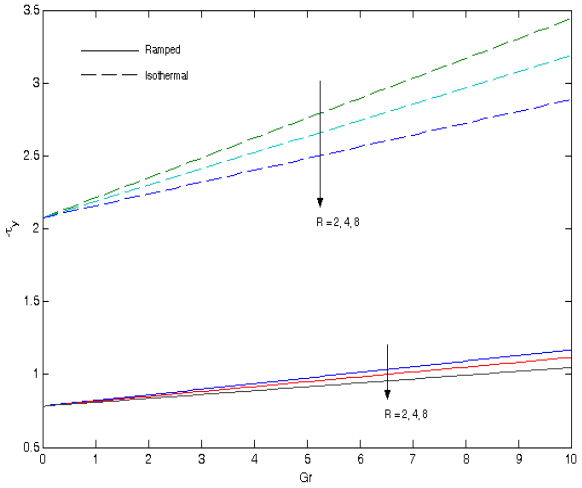

Fig 16: Shear stress τ_y for different R when $Pr = 0.71$, $K^2 = 2$, $\tau = 0.5$ and $Gr = 5$

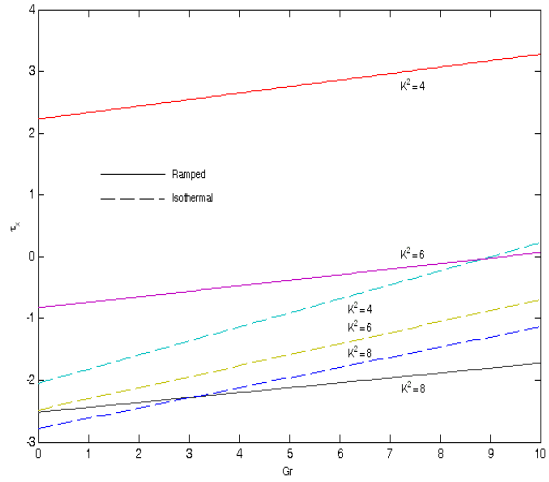

Fig 17: Shear stress τ_x for different K^2 when $Pr = 0.71$, $Gr = 5$, $\tau = 0.5$ and $R = 2$

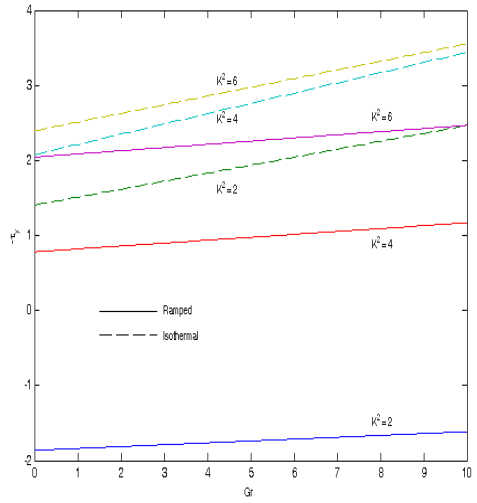

Fig 18: Shear stress τ_y for different K^2 when $Pr = 0.71$, $Gr = 5$, $\tau = 0.5$ and $R = 2$

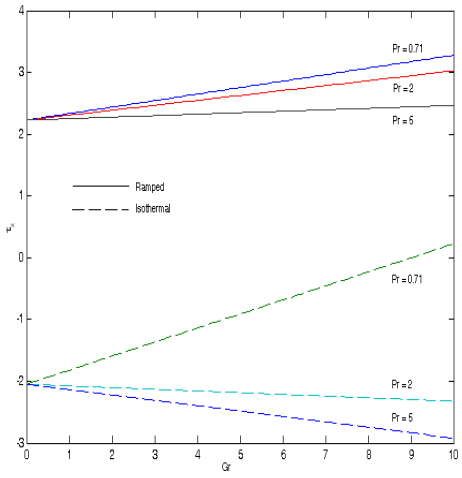

Fig 19: Shear stress τ_x for different Pr when $K^2 = 2$, $Gr = 5$, $\tau = 0.5$ and $R = 2$

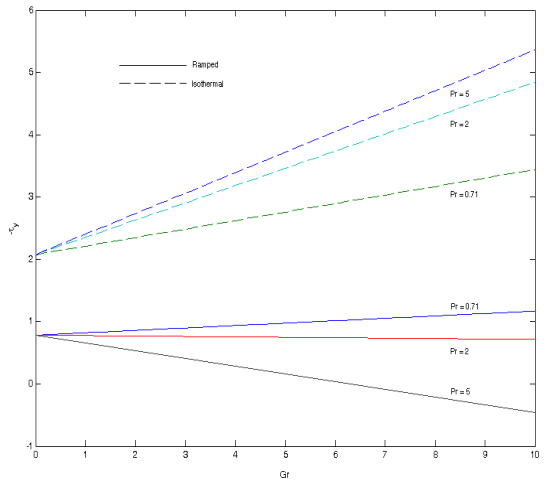

Fig 20: Shear stress τ_y for different Pr when $K^2 = 2$, $Gr = 5$, $\tau = 0.5$ and $R = 2$

4. CONCLUSION

We investigate the combined effects of rotation and radiation on unsteady hydrodynamic flow of a viscous incompressible radiative fluid past an impulsively started vertical plate with ramped plate temperature. It is seen that the radiation parameter has a retarding influence on the velocity field for the ramped plate temperature as well as the isothermal plate. The fluid temperature θ decreases with an increase in radiation parameter R for the ramped plate temperature as well as the isothermal plate. An increase in Prandtl number Pr leads to fall in the fluid temperature θ for the ramped plate temperature as well as the isothermal plate. For the ramped plate temperature as well as the isothermal plate, The velocity field components decrease and they have oscillatory nature away from the plate with an increase in rotation parameter K^2. The absolute value of shear stress τ_x due to the primary flow at the plate $(\eta = 0)$ increases whereas the absolute value of the shear stress τ_y due to the secondary flow at the plate $(\eta = 0)$ decreases with an increase in radiation parameter R for the ramped plate temperature as well as isothermal plate. Further, the rate of heat transfer $-\theta'(0)$ increases with an increase in radiation parameter R.

5. REFERENCES

[1] Das, U. N, Deka, R.K. and Soundalgekar, V. M. 1996. Radiation effects on flow past an impulsively started vertical infinite plate. J. Theo. Mech. 1, 111-115.

[2] Hossain, M.A. and Takhar, H.S. 1996. Radiation effects on mixed convection along a vertical plate with uniform surface temperature. Heat and Mass Transfer. 31, 243-248.

[3] Raptis, A. and Perdikis, C.(1999). Radiation and free convection flow past a moving plate. Int. J. App. Mech. Engg, 4: 817-821.

[4] Revankar, S.T. 2000. Free convection effect on flow past an impulsively started of oscillating infinite vertical plate. Mech. Res. Commun. 27, 241-246.

[5] Li, J., Ingham, D.B. and Pop, I. 2001. Natural convection from a vertical flat plate with a surface temperature oscillation. Int. J. Heat Mass Transfer. 44(12), 2311-2322.

[6] Pathak , G., Maheshwari, C.H. and Gupta, S.P. 2006. Effects of radiation on unsteady free convection flow bounded by an oscillating plate with variable temperature. IJAME. 11 (2), 371-382.

[7] Prasad, V.R., Reddy, N.B. and Muthucumaraswamy, R. 2007. Radiation and mass transfer effects on two- dimensional flow past an impulsively started infinite vertical plate. Int. J. Thermal Science. 46(12), 1251- 1258.

[8] Suneetha, S., Bhasker Reddy, N. and Ram Chandra Prasad, V. 2009. Radiation and mass transfer effects on MHD free convection flow past an impulsively started isothermal vertical plate with dissipation. Thermal Science. 13(2), 171-181.

[9] Muralidharan, M. and Muthucumaraswamy, R. 2010. Thermal radiation on linearly accelerated vertical plate with variable temperature and uniform mass flux. Indian J. Sci. Tech. 3(4),398-401.

[10] Rajesh, V. 2010. Radiation effects on MHD free convection flow near a vertical plate with ramped wall temperature, Int. J. Appl. Math. Mech. 6 (21), 60-77.

[11] Das, S., Jana, M. and Jana, R. N. 2011. Radiation effect on natural convection near a vertical plate embedded in porous medium with ramped wall temperature. Open J. Fluid Dynamics. 1, 1-11.

[12] Anuar, I., Yacob, N.A. and Bachok, N. 2011. Radiation effects on the thermal boundary layer flow over a moving plate with convective boundary condition. Meccanica, DOI 10.1007/s11012-010-9338-4.

[13] Chandrakala, P. 2011. Radiation effects on flow past an impulsively started vertical oscillating plate with uniform heat flux. Int. J. Dynamics of Fluids. 7(1), 1-7.

[14] Rajput, U. S., Kumar, S. 2011. Rotation and radiation effects on MHD flow past an impulsively started vertical plate with variable temperature. Int. J. Math. Analysis. 5(24), 1155-1163.

[15] Seth, G. S., Nandkeolyar, R. and Ansari, M. S. 2011. Effect of rotation on unsteady hydromagnetic natural convection flow past an impulsively moving vertical plate with ramped temperature in a porous medium with thermal diffusion and heat absorption. Int. J. Appl. Math Mech. 7 (21), 52-69.